

## Polymorphic Amorphous and Crystalline Forms of Trehalose

Fabiana Sussich,<sup>†</sup> Ranieri Urbani,<sup>†</sup> Francesco Princivalle,<sup>‡</sup> and Attilio Cesàro<sup>\*†</sup>

Contribution from the Department of Biochemistry, Biophysics and Macromolecular Chemistry and Department of Earth Sciences, University of Trieste, I-34127 Trieste, Italy

Received January 5, 1998

**Abstract:** A characterization has been carried out on the dihydrate and anhydrous crystalline form of trehalose ( $\alpha$ -D-Glucopyranosyl- $\alpha$ -D-glucopyranoside), which is considered anomalous in respect to other disaccharides in conferring to organisms the ability to be dried at high temperatures and then to rehydrate without damaging cellular functions. The thermal dehydration of the dihydrate trehalose,  $T_h$ , has been studied with the aim to rationalize the stability and the kinetically controlled transformations of  $T_h$  into the anhydrous forms. This has been reached by carrying out the dehydration process at different scan rates and by preparing the several polymorphic species. A description is therefore presented of the water–trehalose interaction which controls the thermal stability (or metastability) of the several forms obtained under controlled water depletion. Enthalpy changes and temperatures of transition are also reported and compared with literature data.

## Introduction

The relevance of amorphous and polymorphic states in biological, pharmaceutical, and food science and in the field of polymers has long been recognized. For these states it is important not only to define accurately the thermodynamic transitions (at equilibrium) but also to study the kinetically controlled metastable transformations, which characterize the physical properties of the substances under different experimental conditions.

Among the many sugar molecules that have attracted the attention of scientists and technologists, trehalose seems to be unique in Nature, being involved in the still cryptic process of protecting cellular biomolecules during severe dehydration.<sup>1</sup> Trehalose ( $\alpha$ -D-Glucopyranosyl-(1 $\rightarrow$ 1)- $\alpha$ -D-glucopyranoside, also called mycose) is a non reducing disaccharide that certain living organisms (plants, seeds, invertebrates) synthesize in significant amounts as a natural protectant against water stress. Trehalose can be produced under low humidity conditions, and it permits these organism to be dried at high temperatures and confers to plant and animal cells the ability to survive under extreme conditions of dehydration, a process also called “cryptobiosis” or “anhydrobiosis”, to underline that the organisms do not freeze-dry but dry at high temperatures.<sup>2</sup> The action seems to be due to a stabilizing effect on the membrane structure in the dry state,<sup>3</sup> preventing the biological damage at low temperatures, by binding to proteins and lipid headgroups in the dry bilayers.<sup>4</sup> The presence of trehalose in cryptobionts and also in certain other organisms which are freeze-tolerant has originally induced many workers to concentrate on this molecule

as a cryoprotectant for freeze-drying.<sup>3,5</sup> However, since desert-dwelling cryptobionts do not freeze-dry, it has been also understood that freeze-drying may be unnecessary. In fact, these organisms desiccate in the desert in the hot dry air of summer; therefore, it has been proposed that, if trehalose is responsible for the protection in cryptobiosis, simple air-drying and ambient temperatures can be achieved without molecular damage.

An enormous interest exists in the possibility of using trehalose or other semi-synthetic sugars, as a means of preserving valuable delicate biologically active proteins or living cells at ambient temperature without the need of lyophilization.<sup>4,6</sup> However, understanding of the mechanism of action of trehalose is still incomplete.

Theoretical and experimental works<sup>7</sup> on the details of the molecular features of this anomalous sugar and of the interactions between trehalose and protein macromolecules in solution and during dehydration are ongoing in several laboratories. Trehalose solutions, like those of other sugars, are known to form easily glasses when dried under suitable conditions at biological temperatures.<sup>5</sup> Some authors<sup>7a,b</sup> suggest that trehalose, which has a high glass transition temperature, controls the mobility of water in the course of the glassy state formation. Knowledge about the thermal stability of the several forms which trehalose (dihydrate and anhydrous) can adopt and of specific interactions with water molecules is therefore useful for understanding its mechanism as a protectant agent.

With the above important statements on trehalose properties out of the way, the ubiquitous presence of water in a variety of natural and “artificial” (man-made) products, either as a cocrystallizable component or as a low-moisture plasticizing additive, must also be underlined. These effects of water have

<sup>†</sup> Department of Biochemistry, Biophysics and Macromolecular Chemistry.

<sup>‡</sup> Department of Earth Sciences.

(1) (a) Young S. *New Scientist* **1985**, *10*, 40–44. (b) Fox, K. C. *Science* **1995**, *267*, 1922–1923. (c) Colaco, C.; Kampinga, J.; Roser, B. *Science* **1995**, *268*, 788.

(2) Crowe, J. H.; Crowe, L. M.; Carpenter, J. F.; Aurell Wistrom, C. *Biochem. J.* **1987**, *242*, 1–10.

(3) Carpenter, J. F.; Martin, B.; Loomis, D. H.; Crowe, J. H. *Cryobiology* **1988**, *25*, 372–376.

(4) Lee, C. W. B.; Waugh, J. S.; Griffin, R. G. *Biochemistry* **1986**, *25*, 3737–3742.

(5) Franks, F. *Cryoletters* **1990**, *11*, 93–110.

(6) Lee, C. W. B.; Das Gupta, S. K.; Mattai, J.; Shipley, G. G.; Abdel-Maged, O. H.; Makriyannis, A.; Griffin, R. G. *Biochemistry* **1989**, *28*, 5000–5009.

(7) (a) Crowe, J. H.; Crowe, L. M.; Chapman, D. *Science* **1984**, *223*, 701–703. (b) Ding, S. P.; Fan, J.; Green, J. L.; Lu, Q.; Sanchez, E.; Angell, C. A. *J. Thermal Analysis* **1996**, *47*, 1391–1405. (c) Donnataria, M. C.; Howard, E. I.; Grigera, J. R. *J. Chem. Soc., Faraday Trans.* **1994**, *90*, 2731–2735. (d) Liu, Q.; Schmidt, R. K.; Teo, B.; Karplus, P. A.; Brady, J. W. *J. Am. Chem. Soc.* **1997**, *119*, 7851–7862.

often been the focus of experimental research and of scientific discussion, as water enhances mobility and therefore kinetically controls the transformation of metastable states.<sup>8,9a,b</sup> There is still no general mechanism to quantitatively describe and explain the thermodynamic behavior of these complex systems, although a great exploitation of their technological aspects is pursued. From the scientific point of view, despite the large number of articles with phenomenological descriptions of events occurring under different conditions, quite often one is faced with contradicting assignments of thermal transitions between different physical states or simply with a myriad differing transition temperature data (for the glass transition temperature of sucrose, see for example Table 1 in ref 10). The need for a critical review of this literature data and for sound, comprehensive experiments is extremely great to correctly define even the simple state diagrams of small molecules (see for example ref 11).

Physicochemical data for solid trehalose in some tabulations (see for example ref 12) shows two "melting points" at 91–97 °C and at 203 °C, respectively. The first melting point actually refers to the "dehydration transition" of dihydrate trehalose ( $T_h$  with  $2H_2O$ ), whereas the second refers to the melting of the common, "most-stable" anhydrous form (in this paper referred to as  $T_\beta$ ). Glass transitions have also been reported to occur at 79 °C<sup>13,14</sup> and at 100–115 °C.<sup>7b,12</sup> It seems clear that there is still considerable confusion about trehalose polymorphism. For example, all recent literature has completely overlooked information contained in a note by A. S. Perlin *et al.*<sup>15</sup> on the preparation of two different anhydrous forms obtained by desiccation of the dihydrate at different temperatures.

The present paper reports experimental data showing the existence of the several polymorphs of anhydrous trehalose. The "dynamic" transformation of the dihydrate into anhydrous forms of trehalose, either crystalline or amorphous, is also illustrated. Some very preliminary data were reported in a previous note,<sup>16</sup> providing evidence for some new crystalline forms in addition to the two already studied by X-ray diffractometry.<sup>17</sup> In a subsequent paper (manuscript in preparation), a structural analysis of the crystalline polymorphs of trehalose will be made, which may provide some insight into the structure–stability relations of the molecular architecture of the trehalose crystals.

## Experimental Section

**Materials.** Dihydrate trehalose ( $T_h$ ) was obtained from Sigma Chemical Co. and was used without further purification. The two anhydrous forms,  $T_\alpha$  and  $T_\beta$ , were prepared according to the procedure of Perlin and co-workers<sup>15</sup> for their "a" and "b" anhydrous forms, keeping the dihydrate sample under vacuum at 85 °C for 4 h and at 130 °C for 4 h, respectively.

(8) Angell, C. A. *Science* **1995**, *267*, 1924–1935.

(9) (a) Fito, P.; Mulet, A.; McKenna, B., Eds.; *Water in foods*; Elsevier Applied Science: London, 1994. (b) Roos, Y. *Phase transition in Foods*; Academic Press: San Diego, CA, 1995.

(10) Urbani, R.; Sussich, F.; Prejac, S.; Cesàro, A. *Thermochim. Acta* **1997**, *304/305*, 359–367.

(11) Goldberg, R. N.; Tewari, Y. B. *J. Phys. Chem. Ref. Data* **1989**, *18*, 809–882.

(12) Roos, Y. *Carbohydr. Res.* **1993**, *238*, 39–48.

(13) Green, J. L.; Angell, C. A. *J. Phys. Chem.* **1989**, *93*, 2880–2882.

(14) Levine, H.; Slade, L. J. *Food Eng.* **1994**, *22*, 143–188.

(15) Reisener, H. J.; Goldschmid, H. R.; Ledingham, G. A.; Perlin, A. *Can. J. Biochem. Physiol.* **1962**, *10*, 1248–1251.

(16) Sussich, F.; Urbani, R.; Cesàro, A.; Princivalle, F.; Bruckner, S. *Carbohydr. Lett.* **1997**, *2*, 403–408.

(17) (a) Brown, G. M.; Rohrer, D. C.; Berking, D.; Beevers, C. A.; Gould, R. O.; Simpson, R. *Acta Crystallogr.* **1972**, *B28*, 3145–3158. (b) Taga, T.; Senma, M.; Osaki, K. *Acta Crystallogr.* **1972**, *B28*, 3258–3263. (c) Jeffrey, G. A.; Nanni, R.; *Carbohydr. Res.* **1985**, *135*, 21–30.

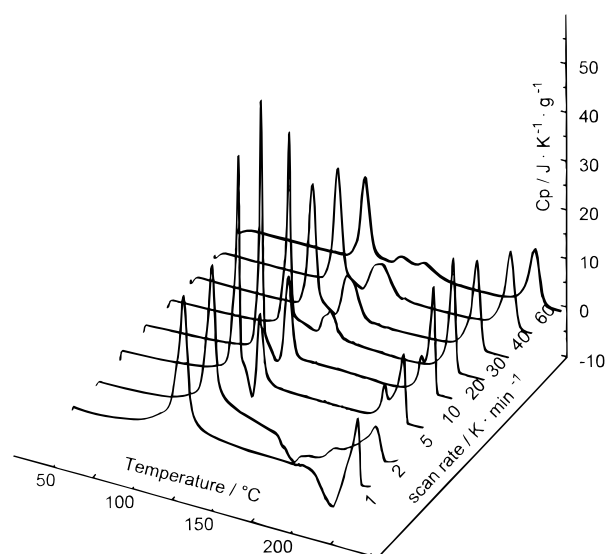


**Figure 1.** DSC thermograms of dihydrated trehalose ( $T_h$ ) from 30 to 230 °C at different scan rates (in  $K \cdot min^{-1}$ , as marked): 1; 2; 5; 10; 20; 30; 40; 60.

**Calorimetric Measurements.** Calorimetric measurements were carried out with a Perkin-Elmer DSC 7 (power compensation) differential scanning calorimeter, connected to a computer via a TAC7/DX Thermal Analysis instrument controller. The calorimeter was equipped also with the Dynamic DSC (DDSC) Accessory and the 7 Series/UNIX DDSC software from Perkin-Elmer was used. The thermal unit was thermostated with an external thermocryostat in which the coolant was kept at  $-30$  °C; a nitrogen flux was used as a purge gas for the furnace. Calibrations were made using indium and zinc at the same scan rates used in the experiments. DSC scans were run on samples weighing between 5 and 15 mg and sealed in pierced aluminum Perkin-Elmer DSC pans; an empty aluminum pan was used as a reference. For the temperature modulated DSC experiments an underlying scan rate of  $1 K \cdot min^{-1}$  was used with a temperature amplitude of  $0.8$  °C and a frequency of  $42$  mHz.

**Thermogravimetry.** Thermogravimetric measurements were carried out with a Perkin-Elmer TGA-7 apparatus with scan rates of 1 and  $20 K \cdot min^{-1}$  on samples covered with pierced aluminum caps in order to simulate the calorimetric experimental conditions; nitrogen at  $30 cm^3 \cdot min^{-1}$  was the purge gas.

**Microscope Observation.** Microscope observation was done on samples placed between cover glass and mounted on a Mettler FP 82 hot stage; the samples were scanned at 1 and  $20 K \cdot min^{-1}$  using a Mettler FP 80 central processor. The microscope used was a Leitz Dialux 22EB with a magnification of  $20\times$ .

**X-ray Diffraction.** X-ray diffraction patterns were obtained on powdered trehalose samples spread out on aluminum plates using a STOE-D500 X-ray diffractometer at room temperature.  $Cu K\alpha$  radiation was obtained through a flat graphite crystal monochromator. Approximately 20 mg were loaded in the sample holder and scanned in the range of  $5$ – $30^\circ$  of  $2\theta$  at  $5$  degree  $2\theta \cdot min^{-1}$  (for samples  $T_h$  and  $T_\beta$ ) and  $1$  degree  $2\theta \cdot min^{-1}$  (for samples  $T_\alpha$  and  $T_\gamma$ ).

## Results

**Dihydrate Trehalose.** Dehydration of dihydrate trehalose ( $T_h$ ) was done in several ways, leading to different forms, either crystalline or amorphous, depending on the different conditions used. The physical transformations were followed with differential scanning calorimetry, thermogravimetry, and direct hot-stage microscopy, using similar protocols, whenever possible. Figure 1 shows thermograms of  $T_h$ , obtained by heating the sample at scan rates ranging from 1 to  $60 K \cdot min^{-1}$ , in the temperature range of  $30$ – $230$  °C. Besides some clear transitions, there are a few remarkable variations in the heating curves as the scan rate is increased.

A slow heating scan (Figure 1, curve marked 1) gives a broad endotherm centered at about 100 °C, clearly associated with the water loss of the crystalline  $T_h$ , as confirmed by the parallel thermogravimetric analysis. Apparently, after dehydration the solid anhydrous trehalose is in an amorphous phase since a flat background in the heat capacity is registered until an exothermic "cold crystallization" occurs at around 180 °C, immediately followed by the melting of the newly formed crystals at  $T > 200$  °C. In all cases, the "cold crystallization" is not reproducibly observed in terms of temperature and associated heat, as is common for nonequilibrium transitions. Microscope observation, carried out on samples placed between cover glass, showed that the multiple shaped hydrated crystals undergo only an internal modification. The crystals themselves tend toward a higher transparency while approaching the transition temperature of dehydration at 100 °C without losing their external morphology. The regular shape of the  $T_h$  crystals remains macroscopically unchanged up to about 135 °C; it is only at about 140 °C that the "solid" sample appears to change its morphological shape ("edge roundness") with an increasing mobility of the phase, although still firm (sticky). The evidence is that an amorphous phase is obtained above 140 °C through the slow heating at ambient pressure of the  $T_h$ . Upon further heating, a crystallization is seen to slowly occur in the liquidus drops (an "undercooled liquid" kinetically unstable) in the form of an agglomeration of unoriented small needles such as a spherulite at the initial growing stage. This new crystallization process, which forms the species already identified as  $T_\beta$  (see below and ref 16), is not yet complete when, slightly above 200 °C, the small crystals melt forming a liquid phase. The microscope observations are reported in Figure 2 and are to be considered in parallel with the above-reported calorimetric data. Consistent results can be seen from the calorimetric experiments where the crystallization process is followed by melting.

In other experiments at increasing scan rate (Figure 1 curves marked 5 and 10) the endotherm centered at about 100 °C becomes sharper and shifts slightly to higher temperatures, as expected. Less obvious is the fact that, right after the dehydration endotherm, already at 5 K min<sup>-1</sup> an exothermic peak appears followed by another (melting ?) endotherm in the temperature range of 120–130 °C. Going to higher scan rates (up to 40 K min<sup>-1</sup>), the crystallization exotherm in the range 110–120 °C becomes less evident, while the subsequent endothermic peak moves to higher temperatures (up to 130–150 °C) and becomes broader. Regardless of the different thermal behavior, all samples (whether undergoing the apparent intermediate crystallization–melting process or not) present a "final" melting to a liquid state at high temperature (above 200 °C) which is characterized at the intermediate scan rates by a double peak.

The difference in the thermal events occurring above 100 °C as a function of the scan rate seems to be a direct consequence of the rate of water loss, which influences the formation of several forms of anhydrous trehalose. The crystallization–melting phenomenon at 110–130 °C has already been observed, and a new crystalline form of trehalose ( $T_\gamma$ ) was reported in the previous note.<sup>16</sup> This fact apparently suggests that the melting transition at 130 °C could indeed be a solid–solid transition, to be consistent with the results at scan rates higher than 10 K min<sup>-1</sup>. However, according to the microscope observations at 20 K min<sup>-1</sup>, the  $T_h$  crystals appear stable up to the dehydration above 95 °C, after which there is trace of some new crystallinity since these new crystals are not regular in shape and disappear when the sample temperature approaches 140 °C.

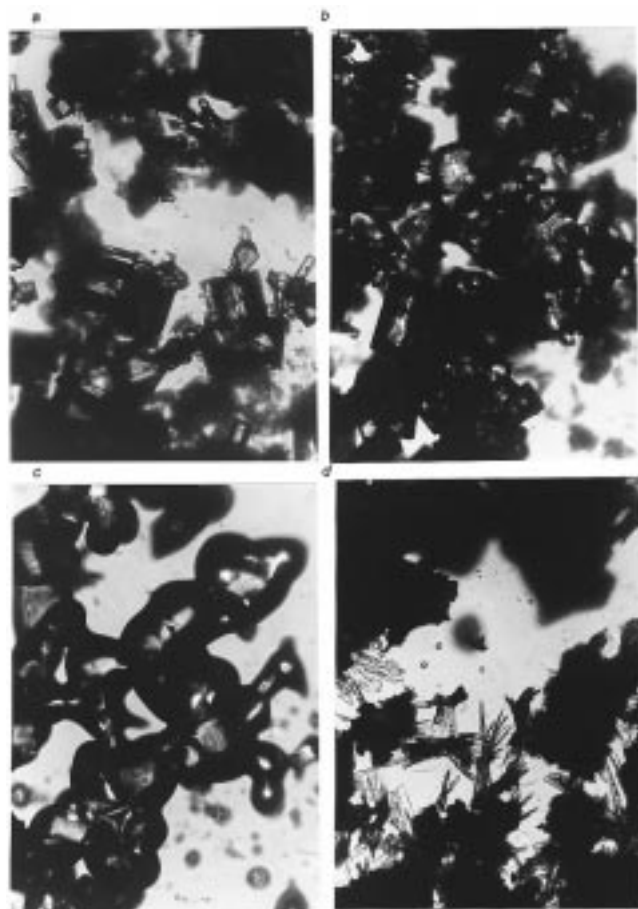


**Figure 2.** Microscope observation of  $T_h$  scanned at 1 K min<sup>-1</sup> at the temperature of (a) 30 °C, (b) 100 °C, (c) 134 °C, and (d) 160 °C.

Above this transition, the "amorphous form" is stable for a small temperature range and then, while still heating, a slow crystallization process is observed. The microscope observation ends with the melting, at about 210 °C, of the anhydrous crystalline form. The optical inspection led us to scrutinize the DSC thermograms more carefully thus attributing the downward shift of the baseline after the second broad endothermic peak to the slow crystallization.

Thermogravimetric experiments were carried out in order to complement the information on the dehydration process. A total of 9.52% of the initial weight is lost in the range around 100 °C at 1 K min<sup>-1</sup>, corresponding to loss of the two water molecules caged in the hydrated structure.<sup>17a,b</sup> At 20 K min<sup>-1</sup>, weight loss is shifted to higher temperatures, with some small but detectable amount of water lost only above 130 °C. However, it should also be mentioned that DSC and TGA cannot reproduce exactly the same experimental conditions.

**Anhydrous Forms: Trehalose- $\beta$  ( $T_\beta$ ), Trehalose- $\alpha$  ( $T_\alpha$ ), Trehalose- $\gamma$  ( $T_\gamma$ ), and the Glassy State.** Two anhydrous forms of the sugar, trehalose- $\beta$  ( $T_\beta$ ) and trehalose- $\alpha$  ( $T_\alpha$ ), were prepared according to the procedure described by Perlin<sup>15</sup> and subjected to the same thermal treatment as the dihydrate trehalose (with heating rates of 1 and 20 K min<sup>-1</sup>). Weight analysis of the samples prepared indicated a stoichiometric loss of 9.52% of the initial weight, which corresponds to the two water molecules of  $T_h$ . An aleatory crystalline form, trehalose- $\gamma$  ( $T_\gamma$ ), was also identified in the DSC runs under appropriate conditions, in addition to the glassy and amorphous states. The relevant transition temperatures and the enthalpy changes of these transitions are given in Table 1.

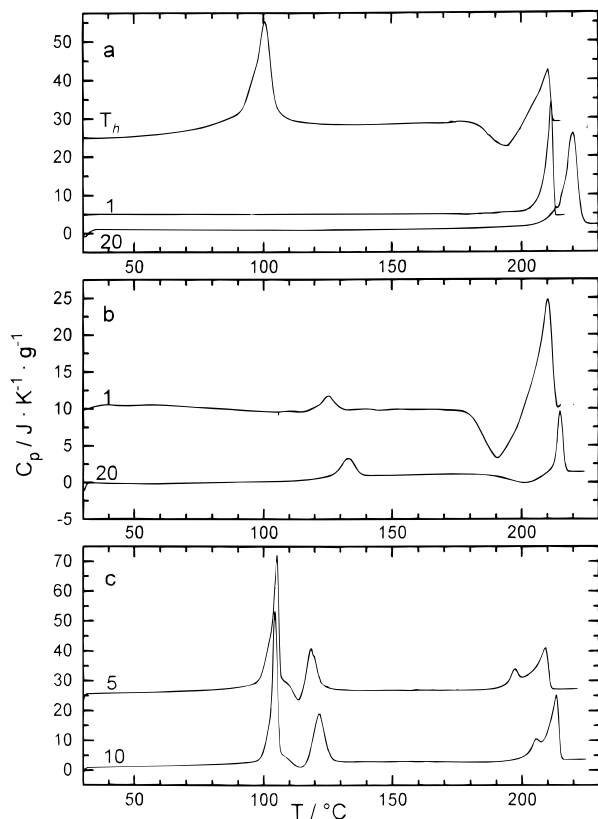


**Figure 3.** DSC thermograms of the several polymorphs of trehalose: (a) trehalose- $\beta$  ( $T_\beta$ ) heated at 1 and 20  $K \cdot min^{-1}$  (for comparison the thermogram of  $T_h$  recorded at 1  $K \cdot min^{-1}$  is also reported); (b) trehalose- $\alpha$  ( $T_\alpha$ ) heated at 1 and 20  $K \cdot min^{-1}$ ; (c) dihydrated trehalose ( $T_h$ ) scanned at 5 and 10  $K \cdot min^{-1}$  showing the crystallization process after the water loss, leading to the formation of trehalose- $\gamma$  ( $T_\gamma$ ).

**A. Trehalose- $\beta$  ( $T_\beta$ ).** Several preparations were made of the “b” form (here called trehalose- $\beta$  ( $T_\beta$ )), using the procedure reported by Perlin. The thermograms were recorded at scan rates of 1 and 20  $K \cdot min^{-1}$ . The features of the thermograms at 20  $K \cdot min^{-1}$  are always identical, from the calorimetric point of view nothing other than a melting occurs at 215  $^\circ C$  (Figure 3). Thermograms recorded at 1  $K \cdot min^{-1}$  have a melting peak above 200  $^\circ C$  with a shoulder, the shape of which is not always reproducible. The  $T_\beta$  form has also been produced from the dihydrate  $T_h$  under different conditions of scan rates, still in the temperature range above 125–150  $^\circ C$ , and its formation is evident from the final melting temperature at  $T = 215 \text{ }^\circ C$ . Comparing the several thermograms, the anhydrous form  $T_\beta$  melts at the same temperature (215  $^\circ C$ ) independently of the different crystallization mechanisms followed for its preparation. The enthalpy change for melting is reported with the other calorimetric data in Table 1. From all thermodynamic results,  $T_\beta$  is the most stable form and its X-ray diffractogram corresponds to the crystalline structure reported in the literature.<sup>17c</sup>

**B. Trehalose- $\alpha$  ( $T_\alpha$ ).** Preparations of the anhydrous “a” form using the method of Perlin<sup>15</sup> were made by keeping the dihydrate sample in a vacuum at 85  $^\circ C$  for 4 h. Here, we refer to it as trehalose- $\alpha$ ,  $T_\alpha$ . Thermograms for this anhydrous  $T_\alpha$  form (Figure 3) were recorded at 1 and 20  $K \cdot min^{-1}$  (weight analysis of the samples showed a decrease of 9.52% due to water loss from the parent  $T_h$ ). At 1  $K \cdot min^{-1}$ ,  $T_\alpha$  displays a first and symmetric endothermic peak at 125  $^\circ C$ , where optical microscopy reveals that the contour of the crystal is no longer well defined. At higher temperatures, cold crystallization is then followed by melting, the latter two transformations also

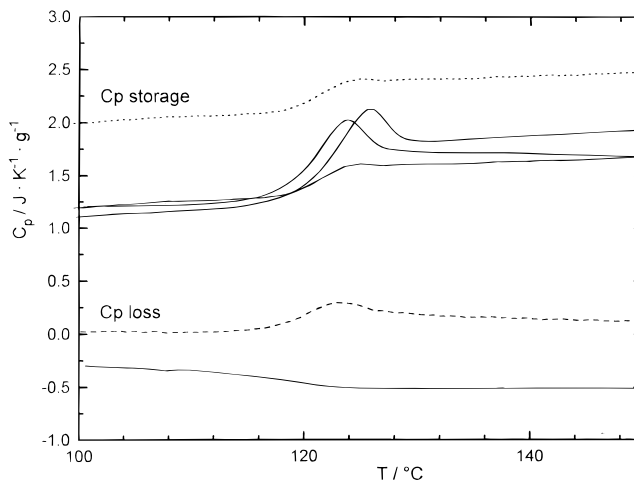


**Figure 4.** Thermograms of amorphous trehalose showing the glass transition both on cooling and on heating; in the figure are also reported the dynamic components ( $C_p$  storage and  $C_p$  loss) obtained by temperature modulation DSC with an underlying scan rate of 1  $K \cdot min^{-1}$  (see text).

confirmed by microscope observation. This kind of behavior is also observed at a scan rate of 20  $K \cdot min^{-1}$  and is consistent with microscope observation, also at 20  $K \cdot min^{-1}$ . Again in this case, after the sample becomes amorphous there is a very slow process of crystallization which does not involve the whole of the specimen’s volume but only a small portion. The melting of this small amount of the crystals (which again resembles needles) occurs at a temperature higher than 215  $^\circ C$ .

**C. Trehalose- $\gamma$  ( $T_\gamma$ ).** The occurrence of this  $T_\gamma$  form was initially shown by the shape of the calorimetric curve for the hydrated crystals at 5–20  $K \cdot min^{-1}$ . The clear presence of an exothermic peak right after water depletion (Figure 3) can only be ascribed to a molecular rearrangement with the formation of a new structural order. The fact that this new crystalline species “melts” at temperatures slightly above its formation (120–130  $^\circ C$ ) also proves that the form is not a stable one. The distinction between the  $T_\gamma$  and  $T_\alpha$  forms is demonstrated not only by the method of preparation and the enthalpy of melting but also by the X-ray diffraction patterns reported below.

**D. Glassy and Amorphous State of Trehalose.** The identification of the glass transition has been made for the solid amorphous form, prepared by rapid cooling of trehalose after melting up to about 220  $^\circ C$ . The thermograms disclose a reproducible step in the heat capacity curve of the amorphous material prepared in this way, as is clearly shown in Figure 4, where both the cooling curve and the heating curve reproduce a jump at about 115–125  $^\circ C$ . This jump is attributed to a glass transition with  $T_g$  (midpoint) = 120  $^\circ C$ . Slightly smaller values have been reported by Roos<sup>12</sup> and by Ding et al.<sup>9</sup> A correct value for the  $T_g$  can only be derived after the enthalpic relaxation peak has been removed, either by analyzing the sample with the temperature modulated mode<sup>4</sup> or by rapidly scanning the freshly prepared amorphous solid, if possible avoiding relaxation events in the  $T_g$  region. Since relaxation peaks seem to be present regardless of the cooling protocols, a temperature modulated scan was carried out using a procedure previously reported for sucrose.<sup>4</sup> The deconvolution of the complex heat capacity gives the two modulation dependent components, the storage heat capacity and the loss heat capacity. The storage heat capacity is the specific heat correlate with several atomic or molecular movements; without any structural changes it proves to be almost identical to the total  $C_p$ . The loss heat capacity instead is linked with dissipation and entropy produc-

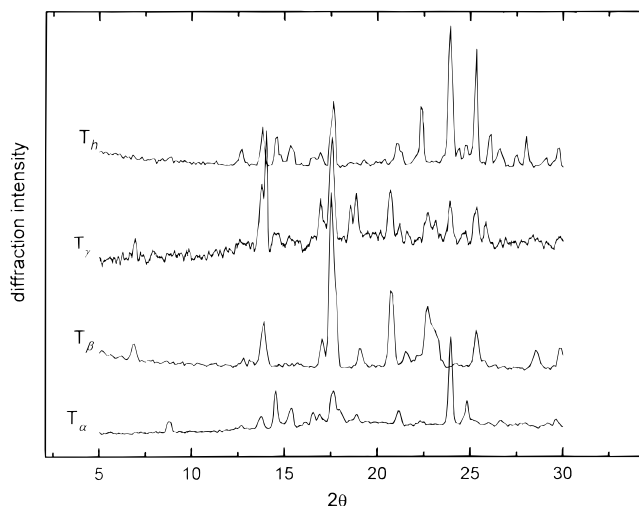


**Figure 5.** X-ray diffraction intensities of the crystalline trehalose forms  $T_h$ ,  $T_\gamma$ ,  $T_\beta$  and  $T_\alpha$ .

tion. Generally speaking the “dynamic curves” give information on phenomena which occur during the time scale of the modulation frequency, the advantage is that thermal effects which happen more or less continuously, not depending on the temperature program, does not appear in all these types of curves. Figure 4 also shows the storage component of the dynamic  $C_p$  obtained by temperature modulation DSC with an underlying scan rate of  $1 \text{ K min}^{-1}$  and a modulation frequency of 42 mHz. The “clean” appearance of a  $T_g$  with a midpoint centered at  $120 \text{ }^\circ\text{C}$  confirms the attribution made by conventional DSC. The  $\Delta C_p$  step of  $0.48 \text{ J K}^{-1} \text{ g}^{-1}$  for the transition is in agreement with the other literature results.<sup>7b,12,13</sup>

**E. X-ray Diffraction.** X-ray diffraction patterns (Figure 5) have been recorded for all forms analyzed (dihydrate  $T_h$ ,  $T_\alpha$ , and  $T_\beta$  trehalose) and also for some sample preparations made in the calorimeter. The latter were used to confirm the presence of amorphous or crystalline forms in specific temperature ranges. The results of  $T_\alpha$  and  $T_\gamma$  shown in Figure 5 have been recorded with high resolution and reproduce the previous preliminary data of our laboratory.<sup>16</sup> Work is being carried out to elucidate the crystal structure of the crystalline forms that are formed from the dihydrate sample.

So far we can say that  $T_\alpha$  and  $T_\beta$  show different X-ray patterns from each other and from that of dihydrate  $T_h$ . In addition, the “transient” form,  $T_\gamma$ , is identified with the crystalline species obtained by “cold crystallization” at  $110 \text{ }^\circ\text{C}$  at intermediate scan rates from the hydrate (curves marked 5, 10, and 20 in Figure 1).

## Discussion

**Dehydration of the Trehalose Hydrate and Formation of Anhydrous Crystalline and/or Amorphous States.** To attempt an interpretation of the several thermal events, one must initially take into account the fact that the water molecules can be removed from the crystalline structure in different ways depending on the scan rate (or other stresses). The scan rate dependence of the enthalpy of dehydration and of the other transitions is shown in Figure 6. At high scan rates, the dehydration process at  $100 \text{ }^\circ\text{C}$  occurs very rapidly (less than 0.5 min over a range of  $10 \text{ }^\circ\text{C}$  at  $20 \text{ K min}^{-1}$ ), sometimes with evident cold crystallization between  $100$  and  $125 \text{ }^\circ\text{C}$ , and a broad peak is observed above  $125 \text{ }^\circ\text{C}$ . At a low scan rate (Figure 6), during a time interval of 20–30 min (corresponding to a width of  $20\text{--}30 \text{ }^\circ\text{C}$  at a rate of  $1 \text{ K min}^{-1}$ ), the dehydration at about

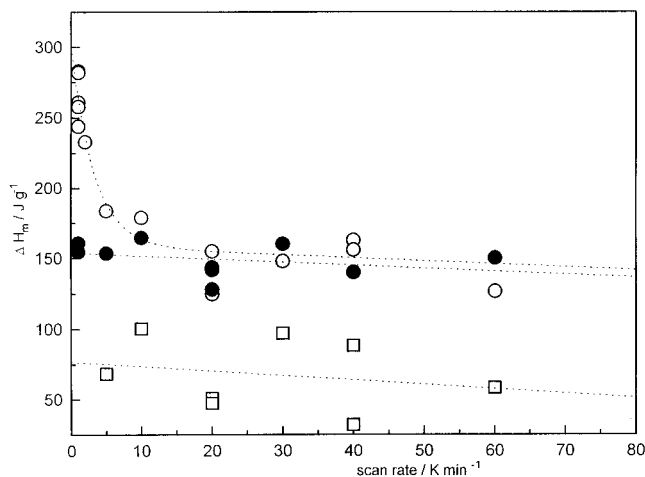


**Figure 6.** Scan rate dependence of the enthalpy of dehydration of  $T_h$  (○) and of melting enthalpy of  $T_\beta$  (●). The data point (□) of the melting enthalpy of  $T_\gamma$ , formed in situ by cold crystallization are also reported.

$100 \text{ }^\circ\text{C}$  occurs when sugar molecules acquire a higher vibrational thermal motion with the simultaneous increase of the apparent molecular volume (the total volume of the dihydrate form without the water molecules). The original molecular order is then easily lost, and a compact disordered state is formed, with a higher specific heat capacity with respect to that of the solid at  $T < 100 \text{ }^\circ\text{C}$ . It must be emphasized that at a slow scan rate ( $1 \text{ K min}^{-1}$ ) the dehydration of  $T_h$  at  $100 \text{ }^\circ\text{C}$  directly produces an amorphous phase and not the glassy form which can be prepared only if the undercooled liquid is quenched at temperatures below the glass transition. In other words, sintering is accomplished by large thermal motions that allow the previously ordered molecular structure to undergo a “quasi-equilibrium” amorphization. Therefore, thermal stresses (as well as mechanical stresses at high temperatures) produce the amorphization of  $T_h$ . However, the particular reason that the process of crystallization–melting in the range of  $110\text{--}130 \text{ }^\circ\text{C}$  does not take place at a very low scan rate ( $1 \text{ K min}^{-1}$ ) is not yet understood and must clearly reside in the dynamics of the transformations which occur at the molecular level upon loss of the water molecules. A delicate kinetic balance exists between the water escaping from the crystalline structure and the structure’s collapse into the disordered state. Unless there is “enough” time or “enough” amorphous water still encapsulated to allow the trehalose molecules to become structurally reorganized, the water depletion may produce either an amorphous state or an unstable open cage of a water-free trehalose network. This “enough–enough” window is not matched at a very low scan rate, and an amorphous anhydrous trehalose is obtained, which is effectively an “undercooled liquid”.

A more detailed interpretation can only be based on the analysis of the molecular architecture in the different crystalline forms (to be presented in the forthcoming paper). In addition, an elucidation of the intriguing and puzzling role of water interaction with trehalose comes from the recent molecular dynamics investigation by Brady et al.,<sup>7d</sup> with the findings that the most stable water–trehalose interactions in solutions resemble those occurring in the hydrate crystalline form.

Whether a glassy state or a rubbery state is reached after a slow water loss apparently depends on whether the transition occurs at  $T < T_g$  or at  $T > T_g$ . Although the presence of the cold crystallization phenomena (Figure 1) is indirect proof of the existence of the glass transition, no conclusion can be drawn from the DSC thermograms alone. It is, however, remarkable that two different cold crystallization processes have been

detected: one found right after the dehydration peak at 100 °C at an intermediate scan rate (5–10 K min<sup>-1</sup>), while another cold crystallization is observed at high scan rates in the region of 150–180 °C before the final melting above 200 °C. Since the first cold crystallization is below the measured  $T_g$  (at 115 °C), it is conceivable that two different unstable states (both glassy?) can be produced in trehalose depending on the method of preparation. To prove the above hypothesis based indirectly on the presence of two different cold crystallizations, one must be able to detect the two glass transitions. However, by taking into account that the original species is a hydrated crystal, the water depletion may be only partially completed and effectively an amorphous “moistured” solid is formed with a much lower  $T_g$  than the  $T_g$  of the anhydrous form. The effect of moisture on the  $T_g$  of carbohydrates can be as high as about 10 K per 1% of water (see for example the most recent data of Blond et al. for sucrose<sup>18</sup> and of Crowe et al. for trehalose<sup>19</sup>). Cold crystallization therefore occurs in a solid which is plasticized by the presence of a small amount of water which has not yet vaporized. When the temperature is raised above the  $T_g$ , the amorphous state can transform from its metastable form to a more stable form, undergoing a “cold crystallization”, and this is seen at  $T = 120$  °C producing  $T_\gamma$  (which is also transformed above 125 °C into a “new ?” amorphous form), and at around 185 °C, which produces the crystalline form  $T_\beta$ , with the final melting (Figure 1, curves 20–60).

The enthalpy of melting of the new crystalline metastable form  $T_\gamma$  has not been reproducibly measured, since the  $T_\gamma$  phase is formed by cold-crystallization and therefore cannot be quantitative. A maximum value of about 100 J g<sup>-1</sup> can be assumed for this transformation. What is important is that the total heat integral over the range from 90 to 140 °C (that is the dehydration plus the crystallization–melting of  $T_\gamma$ ) consistently gives an average value of about 300 J g<sup>-1</sup>, equal to the amorphization of  $T_h$ . Whatever the forms produced after the transitions at 100 and 120–130 °C, they all undergo a very characteristic melting at 215 °C. This melting corresponds to the melting observed in Figure 3 and is ascribed to the crystalline form  $T_\beta$ .

Aside from the reproducible findings reported here, it should be also mentioned that, under several circumstances and without any apparent correlation, some of the thermograms recorded at high scan rates present a slightly different behavior. We have ascribed this random behavior to diverse sampling of the crystal grains and to differences in the water loss through the crystal surface leading to a strong kinetic damping of the thermodynamic transitions, in addition to possible energetic effects due to segregated phases during the transformation. Interpretation of these discrepancies can be done safely only after the dynamic diagram (i.e., with the kinetics of transformation) has been investigated with an appropriate analysis of the crystal sizes.

Before concluding the discussion of the present results on the dehydration of  $T_h$  and the formation of several amorphous and crystalline forms, it is necessary to refer to a paper by Ding et al.<sup>7b</sup> on the vitrification of trehalose by water loss, which appeared while our experiments were in progress. Some of their findings can be interpreted as confirming our results. Unfortunately, despite some relevant qualitative information, this paper contains several internal contradictions in the numerical data (perhaps due to typographical errors) which make it difficult to extract a meaningful understanding of the conditions under

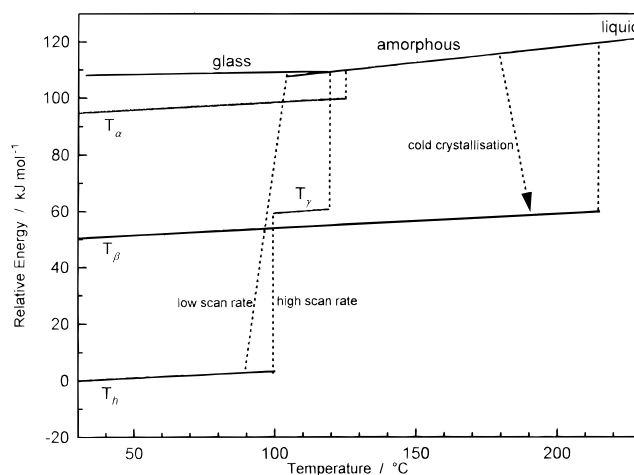


**Figure 7.** Diagrammatic sketch of the temperature/energy transformation of the several trehalose polymorphs.

which the different data were obtained and of the numerical values of the thermal data itself.

**Phase Diagram of the Trehalose Polymorphs.** The relevant information for the various phase transformations of trehalose can be collected in a plot of the enthalpy changes for the several polymorphs identified. Figure 7 shows the temperature stabilities understood so far for the crystalline species  $T_\alpha$ ,  $T_\beta$ ,  $T_\gamma$ , and  $T_h$ , although the slopes of the lines in Figure 7 (that is, the  $C_p$  values) are not quantitative. The above discussion has pointed out the interrelated mechanisms of transformation for the several species. Unlike all of the other forms, the anhydrous  $T_\alpha$  can only be obtained by gently removing the water molecules under vacuum below the threshold of 100 °C. It is reasonable that this rate of water loss does not allow the trehalose structure to relax into a more compact form and that the original sugar architecture is then quenched in an open structure, in which the crystalline motifs can be traced back to the organization of the trehalose molecules in the dihydrate form.

As far as the thermodynamics is concerned, the numerical values of the enthalpy changes of the transitions and of the meltings have been collected in Table 1, together with the temperatures of transition (here conventionally defined as the peak temperatures, given the modification of the shapes of the peaks under the different experimental conditions).

## Conclusions

The results presented here give new insight into the structural polymorphism of trehalose and the complicated kinetics of the transformations. This extended capacity for polymorphism suggests that the molecular explanations for the peculiar properties of trehalose in preserving dry biomaterials<sup>19</sup> must reside in the variability of the energetics of the trehalose interactions, either between sugar molecules or with other molecules, including water. Therefore, the dynamic and viscoelastic properties of the amorphous materials and the glass transition should theoretically be related to the ability of the molecules to establish a high rank of flickering intermolecular interactions. Determining this molecular explanation is simplified by recent experimental results, which using ultrasonic techniques<sup>20</sup> and new NMR techniques<sup>21</sup> have evidenced that trehalose conformation is remarkably stable at different tem-

(18) Blond, G.; Simatos, D.; Catte, M.; Dussap, C. G.; Gros, J. B. *Carbohydr. Res.* **1997**, *298*, 139–145.

(19) Crowe, L. M.; Reid, D. S.; Crowe, J. H. *Biophys. J.* **1996**, *71*, 2087–2093.

(20) Magazù, S.; Migliardo, P.; Musolino, A. M.; Sciortino, M. T. *J. Phys. Chem.* **1997**, *101*, 2348–2351.

(21) Batta, G.; Kover, K. E.; Gervay, J.; Hornyak, M.; Roberts, G. M. *J. Am. Chem. Soc.* **1997**, *119*, 1336–1345.

**Table 1.** Transition Temperatures and Enthalpy Changes

| process                                   | $T/^\circ\text{C}$ (midpoint) | $\Delta H/\text{kJ mol}^{-1}$                       | notes   |
|---|-------------------------------|---|---|
| dehydration: $T_h \rightarrow$ amorphous  | from 100 to 110               | from 108 to 54                                      | scan rate dependence (see Figure 6)                   |
| melting: $T_\beta \rightarrow$ liquid     | 215                           | 52.6  |   |
| melting: $T_\alpha \rightarrow$ amorphous | 126                           | 5.8   |   |
| melting: $T_\gamma \rightarrow$ amorphous | 118–122                       | 23.2  | highest value during the scan by cold crystallization |
| glass transition                          | 125                           | $\Delta C_p = 0.48 \text{ J K}^{-1} \text{ g}^{-1}$ |   |

peratures in dilute and concentrated aqueous solutions, confirming the molecular dynamics studies.<sup>7c,d</sup> New calorimetric experiments in the time–frequency domain can also be useful to clarify the thermodynamics and the crystallization of amorphous into possible nanocrystalline phases.<sup>22,23</sup> Notwithstanding these general, albeit qualitative, views of the protective action of trehalose and other sugars, it seems necessary to have a detailed structural description of the several polymorphs identi-

(22) Sakurai, M.; Murata, M.; Inoue, Y.; Hino, A.; Kobayashi, S. *Bull. Chem. Soc. Jpn.* **1997**, *70*, 847–858.

(23) Salvetti, G.; Tombari, E.; Johari, G. P. *J. Chem. Phys.* **1995**, *102*, 4897–4990.

fied and to pursue suitable theoretical molecular dynamics studies to follow the intermolecular structural fluctuations.

**Acknowledgment** is made for financial support to the Italian Consiglio Nazionale delle Ricerche, CNR (CT9600243), and to the University of Trieste (MURST60%). The authors are grateful to J. W. Brady and S. Bruckner for their interest and fruitful discussions and M. Canetti (Milano) for his kind help with microscopy. F.S. is grateful to Perkin-Elmer Italia S.p.A. for a grant during the initial part of this work.

JA9800479